

# Inhibition of Sphingosine Kinase Activity Enhances Immunogenic Cell Surface Exposure of Calreticulin Induced by the Synthetic Cannabinoid 5-epi-CP-55,940

Jeremy A. Hengst, Asvelt J. Nduwumwami, Wesley M. Raup-Konsavage, Kent E. Vrana, and Jong K. Yun\*

## Abstract

**Background:** Endogenous and synthetic cannabinoids have been shown to induce cancer cell death through the accumulation of the sphingolipid, ceramide (Cer). Recently, we have demonstrated that Cer accumulation enhances the induction of immunogenic cell death (ICD).

**Objectives:** The primary objective of this study was to demonstrate that ( $\pm$ ) 5-epi CP 55,940 (5-epi), a by-product of the chemical synthesis of the synthetic cannabinoid CP 55,940, induces ICD in colorectal cancer (CRC) cells, and that modulation of the sphingolipid metabolic pathway through inhibition of the sphingosine kinases (SphKs) enhances these effects.

**Methods:** A cell culture model system of human CRC cell lines was employed to measure the cell surface and intracellular production of markers of ICD. The effects of 5-epi, alone and in combination with SphK inhibitors, on production of Cer through the *de novo* sphingolipid synthesis pathway were measured by Liquid Chromatography - Tandem Mass Spectrometry (LC/MS/MS)-based sphingolipidomic analysis. Cell surface exposure of calreticulin (ectoCRT), a hallmark of ICD, was measured by flow cytometry. Examination of the effects of 5-epi, alone and in combination with SphK inhibitors, on the intracellular signaling pathway associated with ICD was conducted by immunoblot analysis of human CRC cell lines.

**Results:** Sphingolipidomic analysis indicated that 5-epi induces the *de novo* sphingolipid synthetic pathway. 5-epi dose dependently induces cell surface exposure of ectoCRT, and inhibition of Cer metabolism through inhibition of the SphKs significantly enhances 5-epi-induced ectoCRT exposure in multiple CRC cell lines. 5-epi induces and SphK inhibition enhances activation of the cell death signaling pathway associated with ICD.

**Conclusions:** This study is the first demonstration that cannabinoids can induce the cell surface expression of ectoCRT, and potentially induce ICD. Moreover, this study reinforces our previous observation of a role for Cer accumulation in the induction of ICD and extends this observation to the cannabinoids, agents not typically associated with ICD. Inhibition of SphKs enhanced the 5-epi-induced signaling pathways leading to ICD and production of ectoCRT. Overexpression of SphK1 has previously been associated with chemotherapy resistance. Thus, targeting the SphKs has the potential to reverse chemotherapy resistance and simultaneously enhance the antitumor immune response through enhancement of ICD induction.

**Keywords:** sphingosine kinase; ceramide; 5-epi-CP-55; 940; immunogenic cell death

## Introduction

As the cultural perception of cannabis use changes worldwide, a renewed interest in the medicinal value of natural and synthetic cannabinoids grows rapidly. Numerous purported health benefits have been attrib-

uted to both psychoactive and nonpsychoactive cannabinoids. One effect that is widely reported in the literature is the anticancer activity of cannabinoids (reviewed in Ref.1). We have recently conducted a screen of 370 synthetic cannabinoid compounds to

Department of Pharmacology, Pennsylvania State University College of Medicine, Hershey, Pennsylvania, USA.

\*Address correspondence to: Jong K. Yun, PhD, Department of Pharmacology, Pennsylvania State University College of Medicine, 500 University Drive, Hershey, PA 17033-0850, USA, E-mail:jky1@psu.edu

identify agents that reduced the viability of human colorectal cancer (CRC) cell lines.<sup>2</sup> This screen identified ( $\pm$ ) 5-epi CP 55,940 (hereafter referred to as 5-epi), a by-product of the chemical synthesis of CP 55,940, as the most potent and consistently active compound in the library screen.

Previous studies examining the mechanism of cannabinoid-induced cell death have demonstrated that both synthetic and phytocannabinoids induce *de novo* synthesis of sphingolipids as part of their cell death mechanism.<sup>3-7</sup> *De novo* synthesis of sphingolipids occurs at the cytosolic face of the endoplasmic reticulum (ER). Condensation of serine and palmitic acid by serine palmitoyltransferase (SPT) is the first and rate-limiting step of the synthetic pathway (Fig. 1A).

Multiple steps lead to production of ceramide (Cer) species with variable acyl chain lengths determined by the fatty acyl-CoA specificity of the 6 ceramide synthases (CerS1-6). Cer levels are tightly regulated in cells due to the inherent nature of Cer to induce apoptotic cell death. Cer can be deacylated to release the sphingosine (Sph) backbone, which is rapidly converted to sphingosine-1-phosphate (S1P) by sphingosine kinases 1 and 2 (SphK1/2).

S1P, in direct opposition to Cer, has promitogenic or prosurvival functions both intracellularly and extracellularly (extensively reviewed in Ref.8,9). S1P is a cofactor for several intracellular enzymes, including the E3 ubiquitin ligase activity of TRAF2/6, and acts extracellularly at five G-protein-coupled receptors (S1PR1-5). S1P degradation to phosphoethanolamine and 2-trans-hexadecanal, by S1P lyase, represents an exit path from the sphingolipid metabolic pathway with these products being employed for glycolipid synthesis. Thus, the “on” (SPT activity) and “off” (S1P lyase activity) rates determine the overall levels of sphingolipids in the cell and the relative ratios of Cer to S1P (aka, the “sphingolipid rheostat”) determine cellular fate in response to insult (reviewed in Ref.10).

Historically, the dogmatic view of the mechanism-of-action of cancer chemotherapies has been that they induce apoptosis and hence remain hidden from the innate immune system. However, recent studies have challenged this assertion by demonstrating that certain antineoplastic agents, such as the anthracyclines (e.g., mitoxantrone [MTX]), oxaliplatin, radiation, and photodynamic therapy, can kill cancer cells in a manner that allows them to be recognized as “nonself” by innate and adaptive immune cells through induction of immunogenic cell death (ICD).

ICD-inducing agents stimulate cancer cells to produce a unique cohort of “find me/eat me” signals (dif-

ferent from those observed in cells undergoing apoptosis), termed danger-associated molecular patterns (DAMPs).<sup>11</sup> In contrast, chemotherapeutic agents that are unable to induce ICD fail to promote DAMP release. One of the most important DAMPs is the ER resident chaperone protein, calreticulin (CRT), which is rerouted to the cell surface during ICD. Cell surface exposure of CRT (ectoCRT) acts as an “eat-me” signal on cancer cells to facilitate phagocytosis by dendritic cells (DCs).<sup>12</sup> Other DAMPs that act as “find me” signals have been identified, including autophagy-mediated ATP secretion and the extracellular release of high-mobility group box 1 (HMGB1).<sup>13</sup>

We recently examined the role of Cer accumulation in the induction of ICD by MTX, a well-characterized ICD-inducing agent. We have, for the first time, demonstrated that inhibition of SphK1 and/or SphK2 induces Cer accumulation in response to MTX and enhances the ICD-inducing effects of MTX, including ectoCRT exposure and ATP release.<sup>14</sup> This newly ascribed function of Cer accumulation suggests that other agents that induce Cer accumulation, such as the cannabinoids, may also possess an ability to induce ICD.

Herein, we have further investigated the cellular mechanism associated with the reduction in CRC cell viability induced by the synthetic cannabinoid 5-epi. We demonstrate, for the first time, that 5-epi induces cell death through a mechanism that shares commonalities with ICD. 5-epi induces cell surface exposure of calreticulin (ectoCRT), a well-characterized marker of ICD. Moreover, as observed for other cannabinoids, 5-epi induces *de novo* synthesis of sphingolipids. Inhibition of sphingolipid metabolism, using small-molecule SphK inhibitors, enhances 5-epi-induced ectoCRT supporting a critical role for sphingolipids in the observed effects.

## Materials and Methods

### Reagents and antibodies

5-epi was purchased from Cayman Chemicals (Ann Arbor, MI). PF-543 and z-IETD-fmk were purchased from Selleckchem (Houston, TX). All compounds were prepared in a dimethyl sulfoxide (DMSO) vehicle. Anti-SphK1, anti-CRT, anti-phospho PERK Thr980, anti-ATF6, anti-cFLIP, anti-Full Length Caspase 8, anti-Bap31, anti-Mcl-1, anti-Full Length BID, anti-Full Length Caspase 9, anti-Cleaved PARP, anti-phospho eIF2 $\alpha$  Ser51, and anti-GRP78/BiP were from Cell Signaling Technologies (Beverly, MA). Anti-GAPDH antibodies were from Santa Cruz Biotechnologies (Dallas, TX).

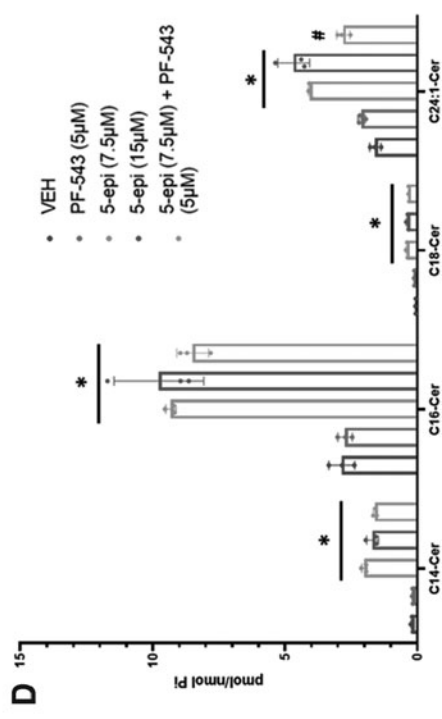
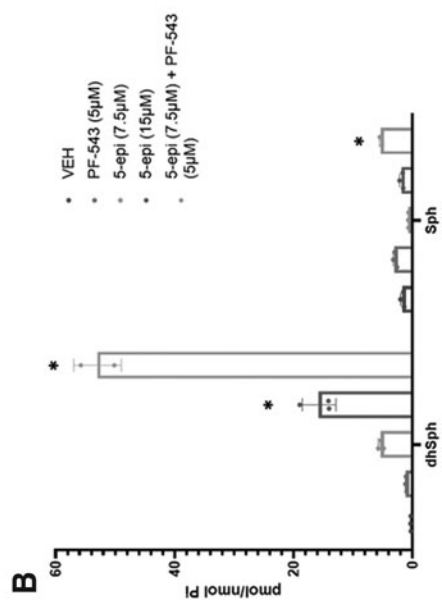
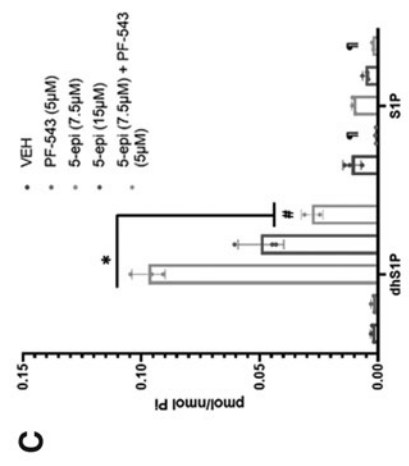


**FIG. 1.** 5-epi induces *de novo* synthesis of long chain Cer species in CRC cells. **(A)** Diagrammatic representation of the *de novo* sphingolipid synthesis pathway and metabolic fates of Cer. Enzymes of the *de novo* synthesis pathway are colored red. Enzymes that attenuate Cer accumulation are colored blue. **(B)** LC/MS/MS analysis of the sphingoid bases, dhSph and Sph, in DLD-1 cells treated with the indicated concentrations of 5-epi, alone or in combination with the SphK inhibitor PF-543 (5 µM), for 48 h (\**p* < 0.001). **(C)** LC/MS/MS analysis of the respective 1-phosphates (\**p* < 0.0001, #*p* < 0.005, †*p* < 0.002). **(D)** LC/MS/MS analysis of major Cer species in DLD-1 cells treated with 5-epi ± PF-543 as indicated, for 48 h (\**p* < 0.0001, #*p* = 0.0057). 5-epi, (±) 5-epi CP 55,940; Cer, ceramide; CRC, colorectal cancer; dhSph, dihydrosphingosine; LC/MS/MS, Liquid Chromatography - Tandem Mass Spectrometry; Sph, sphingosine; SphK, sphingosine kinase.

Anti-SphK2 antibodies were from Proteintech (Rosemont, IL). Anti-phospho IRE1 alpha Ser724 antibodies were from Novus Biologicals (Centennial, CO).

#### Cell lines and culture conditions

Human colorectal DLD-1 (CCL-221), SW480 (CCL-228), SW-620 (CCL-227), RKO (CRL-2577), and HT-29 (HTB-38) were obtained from ATCC, (Manassas, VA). All cells were cultured at 37°C in a humidified atmosphere of 5% CO<sub>2</sub> in Dulbecco's modified Eagle medium (DMEM) supplemented with 10% fetal bovine serum (FBS) and penicillin/streptomycin.

#### Detection of cell surface CRT

For treatment, cells were seeded at  $3 \times 10^5$  cells/well in six-well plates in complete DMEM for 24 h, and then transferred to DMEM containing 5% FBS and penicillin/streptomycin in the presence of treatments for 48 h. Cells were collected by trypsinization, followed by three washes in phosphate buffered saline (PBS) containing 2% FBS, stained with anti-CRT (D3E6) phycoerythrin (PE) conjugated antibody (Cell Signaling Technologies) at 4°C for 1 h, washed as above, and CRT was detected by Muse cell analyzer as previously described.<sup>14</sup>

#### Sphingolipid analysis

DLD-1 cells were treated with 5-epi (7.5 and 15  $\mu$ M) and/or PF-543 (5  $\mu$ M) for 48 h. Cells were collected by trypsinization, pelleted, and washed with PBS and flash frozen. Sphingolipidomic analysis was conducted by the Lipidomic Shared Resource Facility (Medical University of South Carolina, Charleston, SC). Sphingolipid levels were reported as pmoles of sphingolipid per nmole of inorganic phosphate (pmoles/nmole Pi) and were normalized to average fold change relative to the vehicle-treated controls.

#### Whole cell lysate preparation

Total cell lysate was obtained by incubating treated and untreated DLD-1 cells in 1X RIPA buffer (Cell Signaling Technologies), with phosphatase inhibitor cocktail and protease inhibitor tablets (Roche), for 30 min at 4°C and followed by removal of cell debris by centrifugation at 20,000 g at 4°C. Protein concentrations were determined by BCA Assay (Pierce, Waltham MA).

#### Immunoblot analysis

Protein samples were separated on 4–12% NuPAGE gradient gels and transferred to polyvinylidene fluoride membranes under reducing or nonreducing conditions as noted. Membranes were blocked with 5% milk in

Tris buffered saline - Tween 20 (TBS-T) followed by incubation in primary antibodies for 1 h. After three 15-min washes with TBS-T, membranes were incubated in respective secondary antibodies and visualized on X-ray film using Super-Signal West Dura reagents (Pierce, Waltham MA).

#### Statistical analysis

Where appropriate, statistical analysis was performed using one-way analysis of variance (ANOVA) followed by Tukey's multiple comparison test using GraphPad PRISM. Results are reported as average values among replicates with standard deviation (and individual data points).

## Results

5-epi CP 55,940 induces accumulation of Cer species through the *de novo* sphingolipid synthesis pathway

We recently identified 5-epi as a potent agent capable of inducing cell death of CRC cell lines.<sup>2</sup> Numerous studies have revealed an association between *de novo* synthesis of the cytotoxic sphingolipid, Cer, and the mechanism of cell death of  $\Delta^9$ -tetrahydrocannabinol ( $\Delta^9$ -THC) and other cannabinoids. Thus, we initiated these studies to better understand the mechanism of cell death induced by 5-epi.

To determine whether 5-epi CP 55,940 induces *de novo* sphingolipid synthesis, we conducted extensive sphingolipidomic analysis, by Liquid Chromatography - Tandem Mass Spectrometry (LC/MS/MS), in DLD-1 CRC cells. Accumulation of Cer can occur as a result of stimulation of *de novo* synthesis, through the recycling pathway (i.e., catabolism of sphingomyelin species to Cer) or through the salvage pathway (i.e., acylation of Sph to form Cer).

Dihydrosphingosine (dhSph) is exclusively produced through the *de novo* synthesis pathway upstream of generation of dihydroceramide/Cer (Fig. 1A). Thus, accumulation of dhSph is indicative of an increase in the rate of *de novo* sphingolipid synthesis. As shown in Figure 1B, 48 h of 5-epi treatment dose dependently increased the levels of dhSph relative to vehicle (16- to 48-fold,  $p < 0.001$ ). PF-543 (a selective inhibitor of SphK1/2), alone, had minimal effect on levels of dhSph. 5-epi had a much less dramatic effect on levels of Sph with a reduction of Sph at 7.5  $\mu$ M and no change at 15  $\mu$ M (Fig. 1B).

Previous studies have demonstrated that the SphK1/2 can act as antiapoptotic/prosurvival enzymes by converting dhSph to dhSph-1-phosphate (dhS1P).<sup>15,16</sup>

Inhibition of SphK activity, therefore, would be expected to block production of dhS1P synthesis, rerouting dhSph to the enhanced production of dhCer/Cer.

Consistent with this expectation, in DLD-1 cells treated with 5-epi (7.5  $\mu$ M) and PF-543, we observed an  $\sim$ 150-fold increase in dhSph levels versus a 21-fold increase in levels of dhSph with 5-epi (7.5  $\mu$ M) alone (Fig. 1B). This implies that  $\sim$ 85% of the dhSph produced through *de novo* synthesis is being phosphorylated to dhS1P by SphK1/2 and much of that dhS1P is subsequently degraded by S1P lyase. Taken together, the large increase in dhSph relative to Sph is consistent with an increase in the rate of *de novo* sphingolipid synthesis, suggesting that 5-epi CP 55,940 is a functional synthetic cannabinoid.

In support of the conversion of dhSph to dhS1P by SphK1/2, 5-epi alone increased levels of dhS1P (40-fold at 7.5  $\mu$ M and 20-fold at 15  $\mu$ M) as shown in Figure 1C ( $p < 0.0001$ ). In combination with 5-epi (7.5  $\mu$ M), inhibition of SphK1/2 by PF-543 attenuated the production of dhS1P ( $p < 0.005$ ), resulting in the dramatic increase of dhSph observed in Figure 1B. Similarly, PF-543 alone significantly inhibited S1P production relative to vehicle and the 5-epi treatments ( $p < 0.002$ ). PF-543, in combination with 5-epi (7.5  $\mu$ M), also significantly inhibited S1P production relative to 5-epi alone ( $p < 0.002$ ).

Consistent with our recent observation that MTX-induced ICD is mediated through accumulation of Cer species,<sup>14</sup> 5-epi significantly induced accumulation of long chain Cer species (e.g., C14:0, C16:0, and C18:0 Cer), relative to vehicle or PF-543 alone, as shown in Figure 1D ( $p < 0.0001$ ). Levels of very long chain Cer species, including C24:0 and C24:1 Cer, were also significantly elevated, although not to the same extent as the long chain Cer species ( $p < 0.0001$  for 5-epi alone at both concentrations and  $p = 0.0057$  for 5-epi + PF-543 versus vehicle, not significant versus PF-543).

In the presence of the SphK1/2 inhibitor, PF-543 (5  $\mu$ M), we did not observe a further increase in Cer levels, compared to 5-epi alone (7.5  $\mu$ M), even though dhSph levels were elevated by the combined treatment. Whether this is due to increased metabolism of Cer to higher order sphingolipids, such as sphingomyelin or the hexosyl-Cers, or to limited availability of acyl-CoAs for additional Cer synthesis is unknown.

#### SphK inhibition enhances 5-epi CP 55,940-induced ectoCRT

Our recent studies indicated that accumulation of Cer is associated with the induction of ICD by the anthra-

cycline, MTX, through the recycling pathway of Cer generation. Whether these effects are compound specific, or a general feature of the therapy-induced accumulation of Cer has not been examined. Thus, given that 5-epi induced accumulation of Cer, we next determined whether it could also induce markers of ICD in CRC cells.

ICD is determined *in vitro* by the production of DAMPs in response to therapeutic treatment. The best studied of the DAMPs is the relocalization of the normally ER luminal protein, CRT, to the extracellular surface of the plasma membrane (ectoCRT). ectoCRT acts as an “eat-me” signal facilitating engulfment by dendritic/antigen-presenting cells. We previously developed a simple flow cytometry-based assay to determine the ectoCRT/production of ectoCRT.<sup>14</sup>

We next examined whether 5-epi alone, at concentrations close to the reported IC<sub>50</sub> in DLD-1 cells,<sup>2</sup> could induce production of ectoCRT. As shown in Figure 2A, 5-epi, alone, induced a significant dose-dependent increase in cell surface staining of ectoCRT relative to vehicle treatment ( $p < 0.0001$ ). In our previous studies, inhibition of SphKs enhanced MTX-induced Cer accumulation and production of ectoCRT.<sup>14</sup> Although we did not observe such an increase in Cer production with the combination of 5-epi and the SphK inhibitor PF-543, we examined whether PF-543 could enhance the production of 5-epi-induced ectoCRT. In the presence of PF-543, there was a modest, but not statistically significant, increase in ectoCRT exposure with SphK inhibition.

To extend these observations, we also examined the effects of 5-epi alone and in combination with PF-543 in multiple CRC cell lines. SW-480 and SW-620 CRC cell lines are derived from the primary and secondary tumors of a single patient.<sup>17</sup> As shown in Figure 2B, 5-epi alone induced an  $\sim$ sixfold to 10-fold enhancement of ectoCRT levels in SW-480 and SW-620 cells, respectively.

In SW-480 cells, the addition of PF-543 significantly enhanced the production of ectoCRT ( $p = 0.0158$ ), whereas in SW-620 cells, 5-epi alone induced higher levels of ectoCRT relative to SW-480 cells, but PF-543 did not significantly further enhance ectoCRT. Finally, in RKO cells (Fig. 2C), 5-epi alone again enhanced ectoCRT production and the addition of PF-543 significantly enhanced ectoCRT levels ( $p = 0.0007$ ). Together, these data indicate that the effects of 5-epi on production of ectoCRT are not limited to one particular cell line or one particular genetic driver mutation.

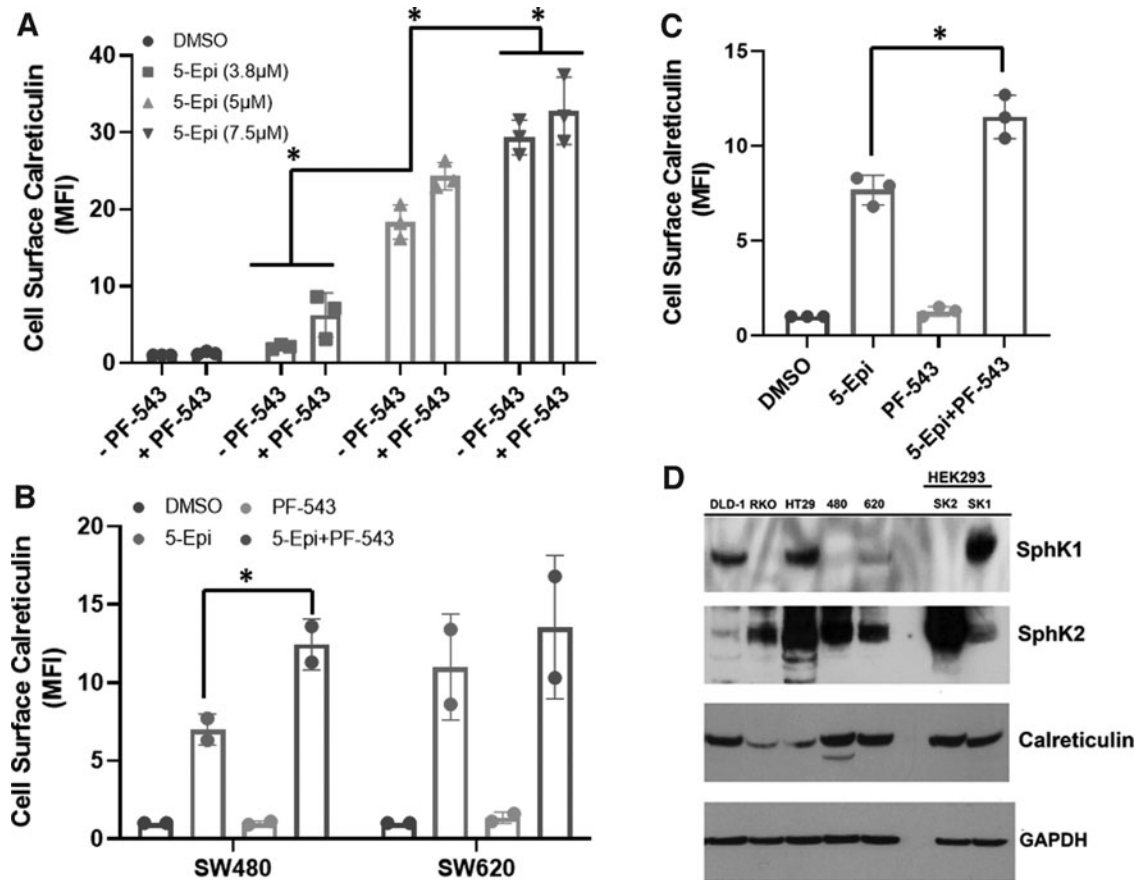


**FIG. 2.** SphK inhibition enhances 5-epi-induced cell surface exposure of calreticulin in CRC cells. **(A)** 5-epi dose-dependently induces cell surface exposure of calreticulin (ectoCRT) in DLD-1 cells, after 48 h of treatment, as determined by flow cytometric analysis using PE conjugated anti-CRT antibodies. Inhibition of SphK1/2 using PF-543 (5  $\mu$ M) enhances 5-epi induced ectoCRT exposure. Results are presented as average MFI normalized to vehicle (DMSO) only controls. (\* $p$  < 0.0001). **(B)** 5-epi (7.5  $\mu$ M) induces ectoCRT in SW-480 and SW-620 CRC cell lines, after 48 h of treatment. PF-543 significantly enhances ectoCRT exposure in SW-480 cells (\* $p$  = 0.0158). **(C)** 5-epi (7.5  $\mu$ M) induces ectoCRT in RKO CRC cells, after 48 h of treatment and PF-543 significantly enhances ectoCRT exposure (\* $p$  = 0.0007). **(D)** Representative western blots of CRC cell lines profiling expression of SphK1, SphK2, CRT and GAPDH (individual western blots) using the indicated antibodies. GAPDH was included as a loading control. HEK293 cell lines stably over-expressing SphK1 and SphK2 were employed as positive antibody controls ( $n$  = 3). CRT, calreticulin; DMSO, dimethyl sulfoxide; ectoCRT, cell surface exposure of CRT; MFI, mean fluorescent intensity; PE, phycoerythrin; SphK1/2, sphingosine kinases 1 and 2.

While the overall trend among the various CRC cell lines was that 5-epi induced ectoCRT, the variability in response to PF-543 led us to consider that the relative protein expression of SphK1 and SphK2 might contribute to the response of cells to PF-543 treatment. Thus, we examined the endogenous expression levels of SphK1 and SphK2 among the cell lines in our panel, by Western blot analysis.

As shown in Figure 2D, although the different cell lines had varying levels of SphK1 and SphK2 protein expression, there was no correlation of the expression of these proteins and the response to either 5-epi alone or to the presence or absence of a significant enhancement in ectoCRT production by the addition of PF-543. We also examined the expression of CRT

and again did not observe any generalizable association to ectoCRT production, indicating that many factors likely affect the production of ectoCRT. HEK293 cell lines overexpressing SphK1 (SK1) and SphK2 (SK2), described previously,<sup>18</sup> were included as positive controls for SphK protein detection.

#### SphK inhibition enhances 5-epi-induced dimerization of ectoCRT

We recently demonstrated that ectoCRT is a disulfide-linked dimer localized to the plasma membrane lipid raft in response to MTX treatment.<sup>14</sup> Importantly, we further demonstrated that SphK inhibition enhanced MTX-induced ectoCRT dimerization. Having established that 5-epi can induce cell surface exposure of ectoCRT, we next examined the oligomeric state of ectoCRT in response to 5-epi under nonreducing conditions.

As shown in Figure 3A, at 7.5  $\mu\text{M}$ , 5-epi alone did not alter the oligomeric state of CRT in whole cell lysates. At 10  $\mu\text{M}$ , 5-epi was able to induce an almost complete shift of cellular CRT from the monomeric state to a dimeric state. Consistent with our previous results, PF-543 enhanced the oligomerization of CRT in the presence of 7.5  $\mu\text{M}$  5-epi, while having no effect on CRT multimerization, alone. The results indicate that dimerization and/or higher order oligomerization of CRT may be a general feature of agents that induce ICD.

#### SphK inhibition enhances 5-epi-induced ICD signaling

The intracellular mechanism associated with MTX-induced production of ectoCRT was examined by Panaretakis et al.<sup>19</sup> They specifically demonstrated that caspase 8 (Casp8) activation and cleavage of the Casp8 substrate, Bap31, were required for cell surface exposure of ectoCRT. We next characterized the mechanism of 5-epi-induced production of ectoCRT. As shown in Figure 3B, 5-epi-induced production of ectoCRT is dependent on the activity of Casp8 as the selective inhibitor z-IETD-fmk (10  $\mu\text{M}$ ) reduced cell surface exposure of ectoCRT in response to 5-epi alone and in the presence of PF-543 ( $p=0.0206$ ).

MTX-induced ICD is intimately associated with ER stress and activation of the unfolded protein response (UPR). Indeed, one arm of the UPR, activation of protein kinase RNA-like ER kinase (PERK), leads to phosphorylation of eukaryotic initiation factor 2 alpha (eIF2 $\alpha$ ) in response to MTX and eIF2 $\alpha$  phosphorylation (Ser51) has been determined to be pathognomonic to the induction of MTX-induced ICD.<sup>20</sup> Thus,

we examined the effects of 5-epi on UPR pathways. Interestingly, as shown in Figure 3C, 5-epi reduced activity/expression of all three arms of the UPR, including activation of PERK and IRE1 $\alpha$  and the expression of ATF6 at high concentrations (10  $\mu\text{M}$ ), suggesting that 5-epi does not induce ER stress.

These effects were not observed at lower concentrations (7.5  $\mu\text{M}$ ), but the addition of PF-543 to 7.5  $\mu\text{M}$  5-epi yielded similar changes to higher 5-epi doses. Although PERK signaling was inhibited by 5-epi (10  $\mu\text{M}$ ) or 5-epi + PF-543 (7.5 + 5  $\mu\text{M}$ ), we did observe a dramatic increase in phosphorylation of eIF2 $\alpha$ , suggesting that eIF2 $\alpha$  phosphorylation may still be required for 5-epi-induced ICD. PERK is one of four kinases known to phosphorylate eIF2 $\alpha$  at Ser51 (PERK [PKR-like ER kinase], the others are PKR [protein kinase double-stranded RNA dependent], GCN2 [general control nonderepressible-2], and HRI [heme-regulated inhibitor]), suggesting that 5-epi could induce ICD through activation of alternative pathways that are not typically associated with ER stress signaling.

To better characterize the signaling mechanism by which 5-epi induces ectoCRT exposure, we next examined the status of proteins associated with Casp8 activation. As shown in Figure 3D, 5-epi dose dependently induced the depletion of the endogenous inhibitor of Casp8, cellular FLICE inhibitory protein (cFLIP). Addition of PF-543 to 7.5  $\mu\text{M}$  5-epi enhanced the depletion of c-FLIP relative to 5-epi alone. The depletion of c-FLIP was associated with activation of Casp8, judged by a decrease in full-length (inactive) Casp8, and cleavage of the Casp8 substrate Bap31 and depletion of the antiapoptotic Bcl-2 family protein, Mcl-1.

We also observed cleavage/activation of another Casp8 substrate, BH3 interacting-domain death agonist (BID), judged by the decrease in levels of full-length BID. BID is a BH3-only protein of the Bcl-2 family, typically associated with induction of intrinsic, mitochondria mediated, apoptosis. Interestingly, despite near full conversion of BID to tBID, we observed only minor activation of caspase 9 (Casp9), the effector caspase associated with mitochondria-mediated apoptosis.

Consistent with the activation of Casp8/9, we observed cleavage of poly (ADP-ribose) polymerase (PARP), a substrate of the executioner caspases, Casp3/7, and an indicator of terminal cell death. Together, these results indicate that 5-epi initiates a cellular death mechanism consistent with the mechanism observed for MTX-induced ectoCRT production, suggesting that 5-epi induces *bona fide* ICD.

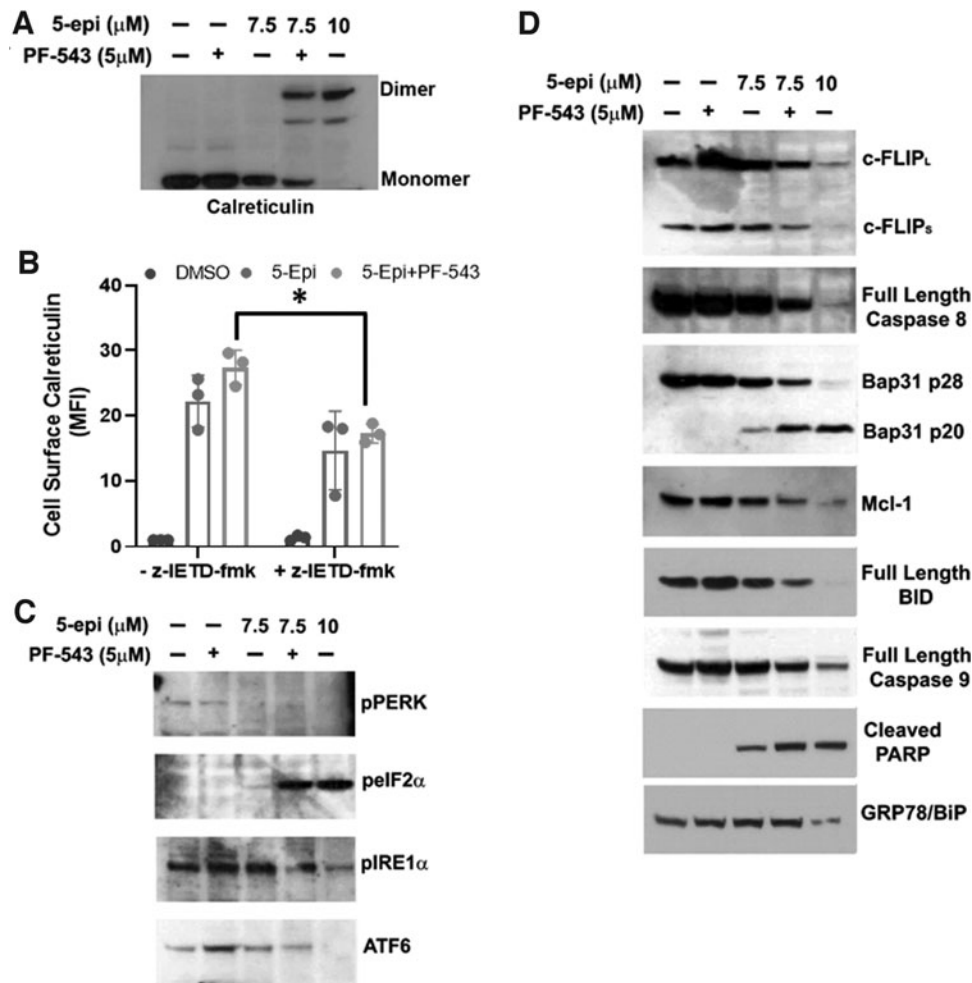


**FIG. 3.** 5-epi attenuates ER stress/UPR and induces ICD signaling pathways in a Casp8-dependent manner in CRC cells. **(A)** The oligomeric state of CRT was examined by nonreducing SDS-PAGE and Western blot analysis of DLD-1 whole cell lysates treated as indicated for 48 h. Representative blot of results from three independent experiments. **(B)** 5-epi-induced ectoCRT exposure is attenuated by inhibition of Casp8 activity (z-IETD-fmk,  $10\ \mu\text{M}$ ) in DLD-1 cells, after 48 h of treatment, as determined by flow cytometric analysis using PE conjugated anti-CRT antibodies. Results are presented as average MFI normalized to vehicle (DMSO)-only controls. ( $*p = 0.0206$ ). **(C)** DLD-1 cells were treated with the indicated concentrations of 5-epi and PF-543 for 48 h. 5-epi at high concentrations ( $10\ \mu\text{M}$ ) and in combination with PF-543 ( $5\ \mu\text{M}$ ) at lower concentration ( $7.5\ \mu\text{M}$ ) reduces activity/expression of the UPR markers PERK, IRE1 $\alpha$ , and ATF6 as determined by Western blot analysis with the indicated antibodies. Phosphorylation of eIF2 $\alpha$  at Ser51 is increased by 5-epi alone ( $10\ \mu\text{M}$ ) or in combination with PF-543 as indicated by Western blot analysis using phosphoselective antibodies. Representative blots of results from three independent experiments. **(D)** Western blot analysis of the signaling pathway associated with ICD in DLD-1 cells treated with 5-epi and PF-543 at the indicated concentrations, for 48 h, using the indicated antibodies. GRP78/BiP serves as a loading control. Representative blots of results from three independent experiments. Casp8, caspase 8; eIF2 $\alpha$ , eukaryotic initiation factor 2 alpha; ER, endoplasmic reticulum; ICD, immunogenic cell death; PERK, protein kinase RNA-like endoplasmic reticulum kinase; UPR, unfolded protein response.



## Discussion

5-epi is a by-product of the synthesis of the nonselective, cannabinoid receptor (CB<sub>1</sub>/CB<sub>2</sub>R) agonist, CP 55,940 (Pfizer). CP 55,940 is structurally similar to the phytocannabinoid, cannabidiol (CBD). In our previous study, 5-epi was ~twofold to threefold more potent than either CP 55,940 or CBD across a collection of CRC cancer cells.<sup>2</sup> This observation prompted us to more closely examine the mechanism(s) associated with cell death to determine whether 5-epi was acting in a manner consistent with the known effects of cannabinoids.

It has previously been reported that  $\Delta^9$ -THC and other phytocannabinoids and synthetic cannabinoids induce *de novo* synthesis of Cer, in a CB receptor-dependent manner.<sup>3-7</sup> Herein, we demonstrate that 5-epi induces *de novo* synthesis of Cer. Importantly, we recently identified a link between Cer accumulation and induction of ICD.<sup>14</sup> Given that 5-epi induced *de novo* Cer synthesis, we also examined whether 5-epi could induce production of ectoCRT, a marker of ICD. Consistent with our previous observations, 5-epi also induced ectoCRT exposure, which was enhanced by modulation of the metabolism of Cer by inhibition of SphK1/2 (Fig. 4).

Although 5-epi is conformationally different than CP 55,940 (a dual CB<sub>1</sub>/CB<sub>2</sub> agonist), it is probable that 5-epi also acts as a CB receptor agonist. The significant increase in cellular levels of dhSph suggests that 5-epi does, in fact, act as a cannabinoid receptor agonist. At the present time, however, the selectivity of 5-epi for CB<sub>1</sub> and CB<sub>2</sub> is unknown, but must be determined in subsequent studies.

Because the psychoactive effects of cannabinoids are typically associated with engagement of CB<sub>1</sub> receptors, while anti-inflammatory/antipain effects are associated with CB<sub>2</sub> receptor engagement, it would be preferable if 5-epi were selective for CB<sub>2</sub> receptors if further development of 5-epi as an anticancer therapeutic agent was to be pursued. Regardless of the selectivity of 5-epi, numerous groups have reported the development of synthetic CB<sub>2</sub> agonists, as anti-inflammatory/antipain agents.<sup>1</sup> It will be interesting to evaluate the anticancer efficacy of additional agents and correlate their affinity to CB<sub>2</sub> receptors with their IC<sub>50</sub> for induction of cell death.

CP 55,940 was developed by Pfizer in 1974, but never marketed, perhaps due to the potential for psychotropic effects due to engagement of CB<sub>1</sub>Rs. It has, however, become routinely employed as a reference compound for studies of CB receptor agonist/antagonist binding. Studies of the metabolic breakdown of CP 55,940 indicated that it was extensively metabolized by cytochrome P450s through side chain monohydroxylation in a manner similar to that of  $\Delta^9$ -THC.<sup>21,22</sup> Thus, it is likely that 5-epi would be metabolized in a similar manner and would have a relatively short half-life.

Although 5-epi may not be an ideal drug candidate, it can be an effective pharmacological tool compound to better dissect the pathway(s) associated with induction of ICD by synthetic cannabinoid agonists. A better understanding of the targets and pathways associated with CB receptor-induced ICD will guide future CB receptor agonist design tailored toward induction of ICD as anticancer therapeutic agents.

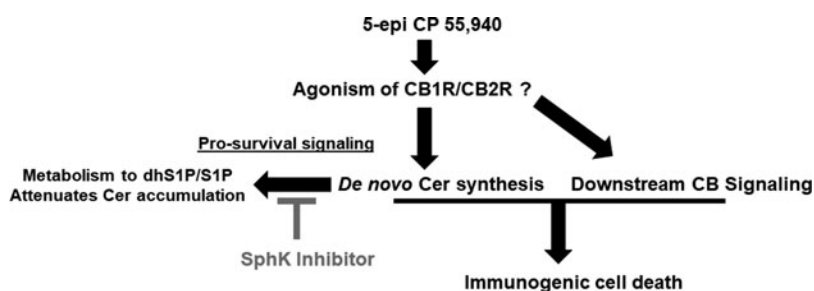


**FIG. 4.** Schematic representation of 5-epi-induced ICD. 5-epi binds to and activates the cannabinoid receptors (CB<sub>1</sub>R and CB<sub>2</sub>R), and/or others. Simultaneously, 5-epi stimulates the *de novo* sphingolipid synthetic pathway to enhance Cer production. SphK1 and/or SphK2 attenuate the accumulation of Cer by conversion of dhSph to dhS1P and conversion of Sph to S1P. Inhibition of the SphKs, using PF-543 or other SphK inhibitors, blocks dhS1P/S1P formation leading to Cer accumulation and enhances the ICD-inducing effects of 5-epi. dhS1P, dhSph-1-phosphate; S1P, sphingosine-1-phosphate.

We demonstrate, for the first time, that a cannabinoid analog can induce the cell surface expression of the DAMP, ectoCRT, suggesting that 5-epi has the potential to induce ICD. Cell surface ectoCRT acts as an “eat-me” signal for engulfment of dying cancer cells by dendritic/antigen-presenting cells. Phagocytosis of ICD-induced dying cancer cells by immature DCs induces their maturation and secretion of cytokines, including IFN $\gamma$ , leading to the induction of an antitumor immune response. The induction of ICD, by 5-epi, suggests that other phytocannabinoids and synthetic cannabinoids, such as CBD, might have the potential to induce ICD.

Finally, this study reinforces our previous observation of a role for Cer accumulation in the induction of ICD and extends this observation to the cannabinoids, agents not typically associated with ICD. Also consistent with our earlier studies, inhibition of the SphKs enhanced the 5-epi-induced signaling pathways leading to ICD and production of ectoCRT.<sup>14</sup>

We further demonstrate that SphK activity greatly attenuates the *de novo* generation of Cer by conversion of dhSph to dhS1P, leading to its subsequent breakdown. Overexpression of SphK1 has previously been associated with chemotherapy resistance through attenuation of *de novo* sphingolipid synthesis.<sup>16</sup> Thus, targeting the SphKs has the potential to reverse chemotherapy resistance and simultaneously enhance the antitumor immune response through the enhancement of ICD induction.

### Author Disclosure Statement

No competing financial interests exist.

### Funding Information

This work was supported by PA Options for Wellness (K.E.V.), the Four Diamonds Fund of the Pennsylvania State University (J.K.Y.), by the Jake Gittlen Memorial Golf Tournament (J.K.Y.), and by the Rite Aid Biomedical Science Program Fund (A.J.N.).

### References

- Shah SA, Gupta AS, Kumar P. Emerging role of cannabinoids and synthetic cannabinoid receptor 1/cannabinoid receptor 2 receptor agonists in cancer treatment and chemotherapy-associated cancer management. *J Cancer Res Ther.* 2021;17:1–9.
- Raup-Konsavage WM, Johnson M, Legare CA, et al. Synthetic cannabinoid activity against colorectal cancer cells. *Cannabis Cannabinoid Res.* 2018;3:272–281.
- Galve-Roperh I, Sanchez C, Cortes ML, et al. Anti-tumoral action of cannabinoids: involvement of sustained ceramide accumulation and extracellular signal-regulated kinase activation. *Nat Med.* 2000;6:313–319.
- Salazar M, Carracedo A, Salanueva IJ, et al. Cannabinoid action induces autophagy-mediated cell death through stimulation of ER stress in human glioma cells. *J Clin Invest.* 2009;119:1359–1372.
- Gustafsson K, Sander B, Bielawski J, et al. Potentiation of cannabinoid-induced cytotoxicity in mantle cell lymphoma through modulation of ceramide metabolism. *Mol Cancer Res.* 2009;7:1086–1098.
- Gomez del Pulgar T, Velasco G, Sanchez C, et al. De novo-synthesized ceramide is involved in cannabinoid-induced apoptosis. *Biochem J.* 2002;363:183–188.
- Khan MI, Sobocinska AA, Brodaczewska KK, et al. Involvement of the CB2 cannabinoid receptor in cell growth inhibition and G0/G1 cell cycle arrest via the cannabinoid agonist WIN 55,212-2 in renal cell carcinoma. *BMC Cancer.* 2018;18:583.
- Sukocheva OA, Furuya H, Ng ML, et al. Sphingosine kinase and sphingosine-1-phosphate receptor signaling pathway in inflammatory gastrointestinal disease and cancers: a novel therapeutic target. *Pharmacol Ther.* 2020;207:107464.
- Sukocheva OA. Expansion of sphingosine kinase and sphingosine-1-phosphate receptor function in normal and cancer cells: from membrane restructuring to mediation of estrogen signaling and stem cell programming. *Int J Mol Sci.* 2018;19. doi:10.3390/ijms19020420.
- Moro K, Nagahashi M, Gabriel E, et al. Clinical application of ceramide in cancer treatment. *Breast Cancer.* 2019;26:407–415.
- Galluzzi L, Vitale I, Warren S, et al. Consensus guidelines for the definition, detection and interpretation of immunogenic cell death. *J Immunother Cancer.* 2020;8:e000337.
- Wiersma VR, Michalak M, Abdullah TM, et al. Mechanisms of translocation of ER chaperones to the cell surface and immunomodulatory roles in cancer and autoimmunity. *Front Oncol.* 2015;5:7.
- Kepp O, Senovilla L, Zitvogel L, et al. Consensus guidelines for the detection of immunogenic cell death. *Oncoimmunology.* 2014;3:e955691.
- Nduwumwami AJ, Hengst JA, Yun JK. Sphingosine kinase inhibition enhances dimerization of calreticulin at the cell surface in mitoxantrone-induced immunogenic cell death. *J Pharmacol Exp Ther.* 2021;378:300–310.
- Berdyshev EV, Gorshkova IA, Usatyuk P, et al. De novo biosynthesis of dihydrosphingosine-1-phosphate by sphingosine kinase 1 in mammalian cells. *Cell Signal.* 2006;18:1779–1792.
- Siow D, Sunkara M, Morris A, et al. Regulation of de novo sphingolipid biosynthesis by the ORMDL proteins and sphingosine kinase-1. *Adv Biol Regul.* 2015;57:42–54.
- Hewitt RE, McMarlin A, Kleiner D, et al. Validation of a model of colon cancer progression. *J Pathol.* 2000;192:446–454.
- Hengst JA, Dick TE, Smith CD, et al. Analysis of selective target engagement by small-molecule sphingosine kinase inhibitors using the Cellular Thermal Shift Assay (CETSA). *Cancer Biol Ther.* 2020;21:841–852.
- Panaretakis T, Kepp O, Brockmeier U, et al. Mechanisms of pre-apoptotic calreticulin exposure in immunogenic cell death. *EMBO J.* 2009;28:578–590.
- Bezu L, Sauvat A, Humeau J, et al. eIF2alpha phosphorylation is pathognomonic for immunogenic cell death. *Cell Death Differ.* 2018;25:1375–1393.
- Thomas BF, Martin BR. Identification of metabolites of CP-55,940 formed in-vitro by mouse livers. *NIDA Res Monogr.* 1989;95:287–288.
- Thomas BF, Martin BR. In vitro metabolism of (–)-cis-3-[2-hydroxy-4-(1,1-dimethylheptyl) phenyl]-trans-4-(3-hydroxypropyl) cyclohexanol, a synthetic bicyclic cannabinoid analog. *Drug Metab Dispos.* 1990;18:1046–1054.

**Cite this article as:** Hengst JA, Nduwumwami AJ, Raup-Konsavage WM, Vrana KE, Yun JK (2022) Inhibition of sphingosine kinase activity enhances immunogenic cell surface exposure of calreticulin induced by the synthetic cannabinoid 5-epi-CP-55,940. *Cannabis and Cannabinoid Research* 7:5, 637–647, DOI: 10.1089/can.2021.0100.

**Abbreviations Used**

5-epi = ( $\pm$ ) 5-epi CP 55,940  
 $\Delta^9$ -THC =  $\Delta^9$ -tetrahydrocannabinol  
BID = BH3 interacting-domain death agonist  
c-FLIP = cellular FLICE inhibitory protein  
Casp8 = caspase 8  
Casp9 = caspase 9  
CB1R/CB2R = cannabinoid receptor 1/2  
CBD = cannabidiol  
Cer = ceramide  
CRC = colorectal cancer  
CRT = calreticulin  
DAMPs = danger-associated molecular patterns  
DCs = dendritic cells  
dhS1P = dhSph-1-phosphate  
dhSph = dihydrosphingosine  
ectoCRT = cell surface exposure of calreticulin  
eIF2 $\alpha$  = eukaryotic initiation factor 2 alpha

ER = endoplasmic reticulum  
GCN2 = general control nonderepressible-2  
HMGB1 = high-mobility group box 1  
HRI = heme-regulated inhibitor  
ICD = immunogenic cell death  
LC/MS/MS = Liquid Chromatography - Tandem Mass Spectrometry  
MTX = mitoxantrone  
PARP = poly (ADP-ribose) polymerase  
PBS = phosphate buffered saline  
PE = phycoerythrin  
PERK = protein kinase RNA-like endoplasmic reticulum kinase  
PKR = protein kinase double-stranded RNA dependent  
S1P = sphingosine-1-phosphate  
SKIs = sphingosine kinase inhibitors  
Sph = sphingosine  
SphK1/2 = sphingosine kinases 1 and 2  
SphKs = sphingosine kinases  
SPT = serine palmitoyltransferase  
UPR = unfolded protein response